ACADEMIA ROMÂNĂ
Revue Roumaine de Chimie
http://web.icf.ro/rrch/

Rev. Roum. Chim.,
2018, *63*(10), 919-929

FOUR NEW COMPLEXES OF Mg(II), Ca(II), Sr(II), AND Ba(II) INDOMETHACIN ANTI-INFLAMMATORY DRUG: SYNTHESIS, PHYSICOCHEMICAL AND ANTIMICROBIAL STUDIES

Fatima A. I. AL-KHODIR

Department of Chemistry, College of Science, Princess Norah bint Abdulrahman University, Riyadh 11671, KSA

Received November 24, 2017

New series of Mg(II), Ca(II), Sr(II) and Ca(II) complexes with indomethacin (*indo*) anti-inflammatory drug have been synthesized. These complexes have been characterized by different physico-chemical techniques like elemental analysis, FT-IR, UV-Vis spectroscopy, ^{1}H-NMR spectroscopy, conductance measurements, and thermo-gravimetric analysis. Spectroscopic studies suggest coordination of all complexes in a regular octahedral arrangement in 2L:1M molar ratio by two O-carboxylate group and four coordinated water molecules in the form of $[M(L)_2(H_2O)_4]$, M metal, L ligand (*indo*). The FT-IR spectra of complexes indicate the involvement of the –COOH group in the complexation after deprotonation as monodentate. The nanoscale range of the prepared complexes was analyzed based on transmittance electron microscopy (TEM). Complexes have been screened for their antibacterial (Gram negative bacteria (*Escherichia coli*), (Gram positive bacteria (*Bacillus subtilis*) and antifungal (*Aspergillus niger* and *Aspergillus flavus*) showing promising antimicrobial biological activity.

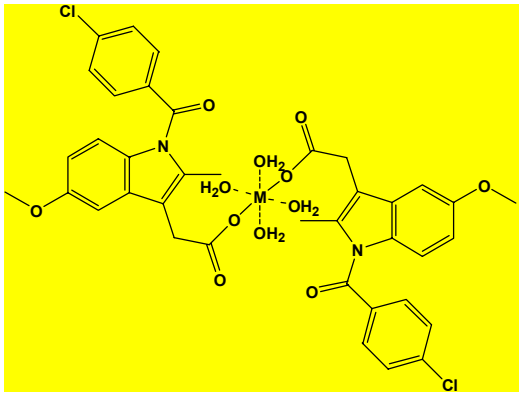

INTRODUCTION

Indomethacin (*indo*, Fig. 1) is one of the most potent of the clinically used non-steroidal anti-inflammatory drugs (NSAIDS) and interferes with prostaglandin synthesis by direct inhibition of the two cyclo oxygenase systems.[1] Indomethacin is used as analgesic and antipyretic but its efficacy is offset by significant incidence of gastrointestinal ulceration and hemorrhage. The absorption of *indo* is associated within minutes.[2] In literature survey, the cooper (II) complexes with NSAID ligands have been a pharmacological properties as an active anti-inflammatory agent. The carboxylate group has an attracted attention because of the diversity of the binding modes.[7] Indomethacin is a mono carboxylic acid which is capable of forming a coordination bond with many metals. In this paper we reported the synthesis and spectral characterizations of Sr(II), Ba(II), Ca(II), and Mg(II) complexes of indomethacin. The complexes have been characterized using IR, ^{1}HNMR and conductivity measurement and biological evaluation of non-transition indomethacin complexes.

RESULTS AND DISCUSSION

1. Elemental analysis and conductance measurements

The results of elemental analysis and physical properties of the *indo* complexes are presented in Table 1. The complexes are stable, insoluble in H_2O

* Corresponding author: fatimaalkhodir@yahoo.com

and are soluble in dimethylsulfoxide (DMSO) and dimethylformamide (DMF) organic solvents. The four isolated solid complexes are [Sr(*indo*)$_2$(H$_2$O)$_4$] (**1**), [Ba(*indo*)$_2$(H$_2$O)$_4$] (**2**), [Ca(*indo*)$_2$(H$_2$O)$_4$] (**3**), and [(Mg(*indo*)$_2$(H$_2$O)$_4$] (**4**), which resulted from interaction between the chloride salts of the Sr^{II}, Ba^{II}, Ca^{II} and Mg^{II} ions and the *indo*-H ligand. Table 1 gives the percentage of observed and calculated data of the carbon, hydrogen, nitrogen and divalent metal(II) ions contents, which are in good agreement with each other.

Molar conductivities of *indo* complexes in DMF solvent (10^{-3} M) were in the range of 7-16 Scm^2mol^{-1}, suggesting them to be of non-electrolyte nature.[8] These data matched with the absence of Cl^- ion evidenced by $AgNO_3$.

2. Infrared spectra

The main infrared bands of M(II)/*indo* are summarized in Table 2 and shown in Fig. 2$_{a,b}$. The *indo* free drug ligand exhibits a very strong absorption band at 1716 cm^{-1} due to stretching vibration of ν(C=O) of free ketonic of carboxylic group.[9] This band is shifted or disappeared in the spectra of its complexes. The major characteristic of the IR spectra is the frequency of the υ_{asym}(COO) and υ_{sym}(COO) stretching vibration. The frequency of these bands depends upon the coordination mode of the carboxylate group. The υ_{asym}(COO) and υ_{sym}(COO) bands appear at 1530-1598 cm^{-1} and 1340-1398 cm^{-1}, respectively.[10] Nakamoto *et al.*[11] have established that if the co-ordination is monodentate, the υ_{asym} (COO) and υ_{sym}(COO) will be shifted to higher and lower frequencies, respectively. Whereas, if the coordination is chelating bidentate or bridging bidentate, both the υ_{asym} (COO) and υ_{sym}(COO) change in the same direction because the bond order of both (C=O) bonds would change by the same amounts. On the basis of these facts and comparison of the υ_{asym}(COO) and υ_{sym}(COO) frequencies of the *indo* complexes by the υ_{asym}(COO) and υ_{sym}(COO) frequencies of sodium carboxylate[10], it can be said that all prepared complexes have a monodentate structure. The stretching broad band of υ(O-H) occurred as expected[10,12] at range 3400-2500 cm^{-1}. It should be mentioned here that these assignments for the bands assigned to coordinated water deformation (ρ_r and ρ_w) molecule fall in the frequency regions (600-800 cm^{-1}) reported for related complexes.[12] The weak or medium intensity were observed in the wave number range 475-560 cm^{-1} and can be assigned to υ(M-O) stretching vibration.

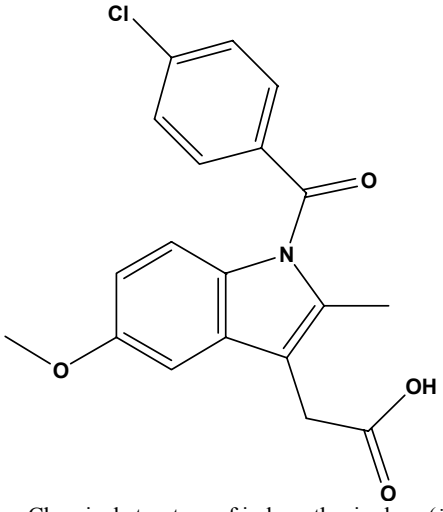

Fig. 1 – Chemical structure of indomethacin drug (*indo*).

Table 1

Elemental analysis and physical data of *indo* complexes

Complex	Content ((calculated) found)				Λ Scm^2 mol^{-1}
	C %	H %	N %	M %	
1	(56.35) 56.21	(4.75) 4.54	(3.46) 3.41	(3.00) 2.96	7
2	(55.28) 55.18	(4.64) 4.56	(3.39) 3.31	(4.85) 4.80	15

Table 1 (continued)

3	(52.27) 52.18	(4.39) 4.32	(3.21) 3.19	(10.03) 9.96	12
4	(49.45) 49.39	(4.15) 4.09	(3.04) 3.00	(14.88) 14.81	16

Table 2

IR frequencies (cm^{-1}) of *indo*-H and its Sr^{II}, Ba^{II}, Ca^{II} and Mg^{II} complexes

Assignments	*indo*-H	Compounds			
		Sr(II)	Ba(II)	Ca(II)	Mg(II)
ν(OH); H_2O	3412	3408	3406	3388	3421
ν(CH) aromatic	3058	2989	2931	2990	2932
$\nu_{as}(CH_2)$	2974	2932		2948	
$\nu_{as}(CH_2)$	2870	-	-	2835	-
ν(COOH)	1716	-	-	-	-
ν(CO) amide	1685	1684	1623	1684	1677
ν_{as}(COO)	1585	1542	1552	1543	1593
ν_s(COO)	1440	1438 1398	1475 1370	1446 1397	1469 1366
δ(CH) + (C-O)	1370	1365 1316	1318	1367 1316	1321
ν_{as}(C-O-C) ρ(CH) aromatic	1274, 1246, 1178, 1129	1267, 1227, 1180, 1144, 1078, 1023	1226, 1147 1080, 1036	1267, 1227 1183, 1144 1078, 1035	1227, 1147 1080, 1029
ν(C-N)	1074			1023	
ν_s(CC)	974	919	918	918	919
δ(CC) ($\rho_r + \rho_w$); H_2O	819	837, 800, 752, 684, 624	835, 787 748, 680	835, 799 752, 682, 624	839, 754 661, 605
ν(M-O)	-	542, 475	596, 476	542, 474	481

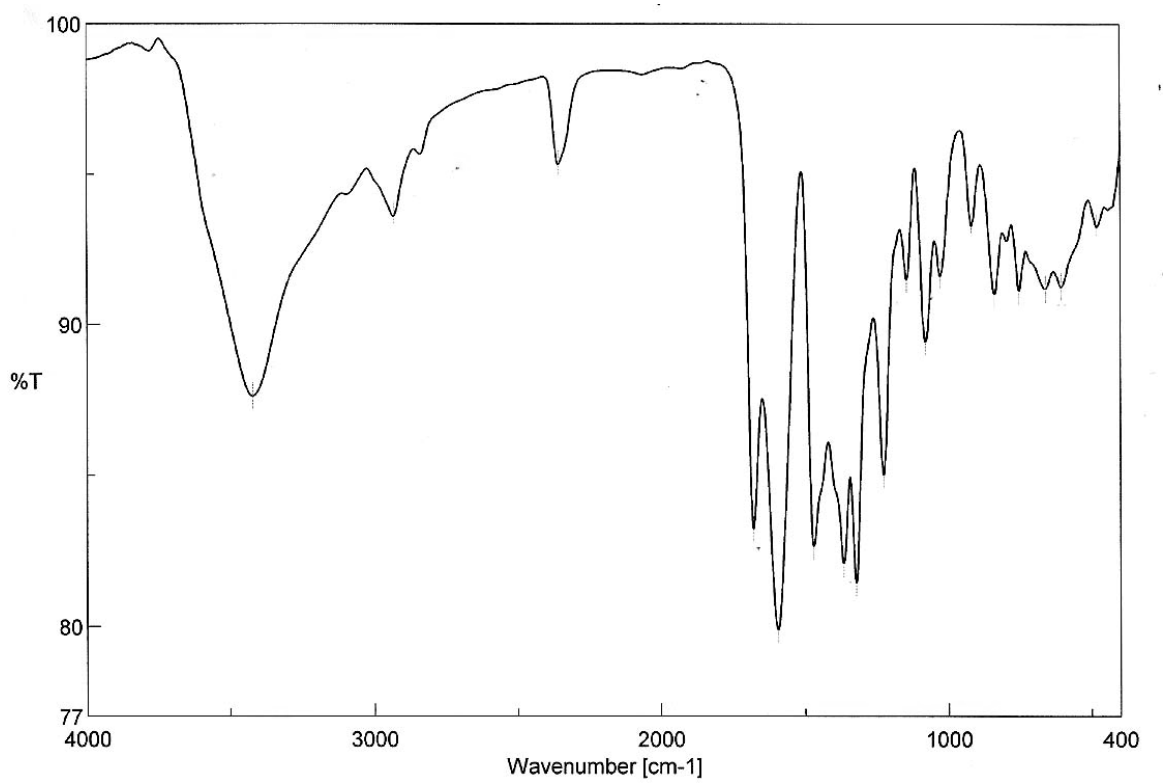

Fig. 2a – FT-IR spectrum of *indo*/Mg^{2+} complex.

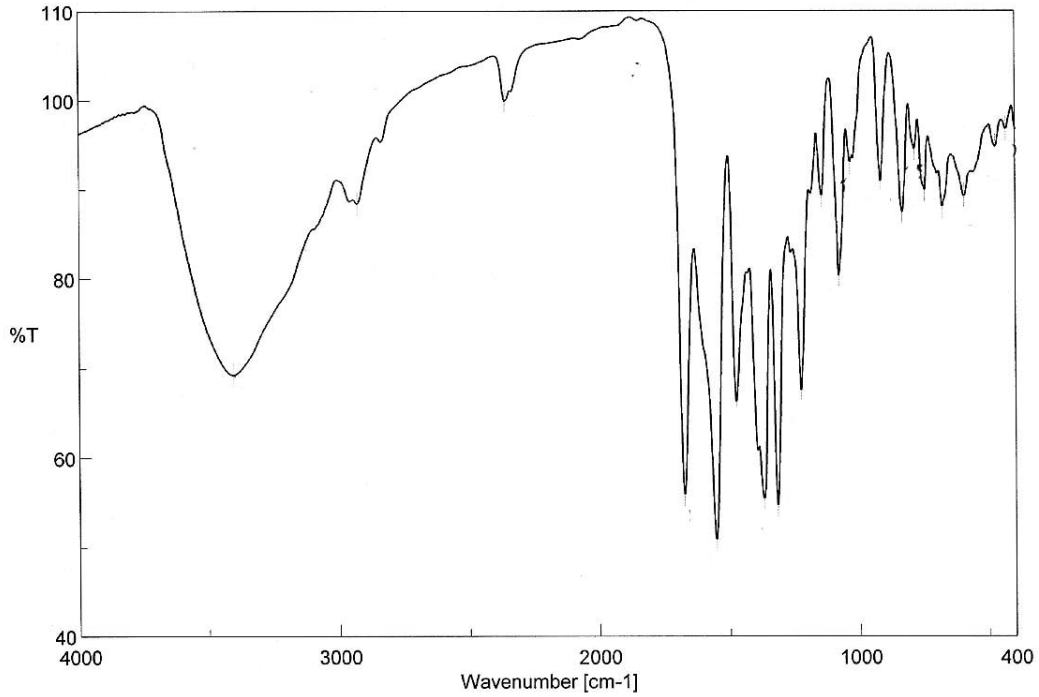

Fig. 2b – FT-IR spectrum of *indo*/Ba^{2+} complex.

3. ^{1}H-NMR spectra

The ^{1}H-NMR spectra for *indo*-H and Sr(II) complex were carried out in DMSO. The ^{1}H-NMR data for free *indo*-H: δ = 11.10 [H, COOH], 2.1 [2H, CH_2], 3.5 [3H, CH_3], 4.1 [3H, $C\underline{H}_3O$], 6.15-7.15 [H, aromatic rings]. The ^{1}HNMR data for the Sr(II)/*indo* solid complex are in agreement with coordination through the carboxylic group by the absence of the H(1) signal in Sr(II) complex and aromatic signals decreased in the intensities, thus showing that the magnetic environment of aromatic ring has changed significantly with coordination. The signal observed at 2.48-2.51 and 3.37 ppm in case of Sr(II) complex, see Table 3 and Fig. 3, are assigned to the coordinated water molecules.

4. UV-Vis spectra and optical band gap

The UV-Vis spectrum of the *indo*-Sr complex show strong absorption band at 304 nm due mainly to intraligand π–π* band as shown in Fig. 4 Concerning *indo* complexes of Mg(II), Ca(II), and Ba(II) metal ions have two strong absorptions around ~ 300 and ~ 375 nm (see Fig. 4) that were attributed to π–π* and n–π* transitions, respectively.

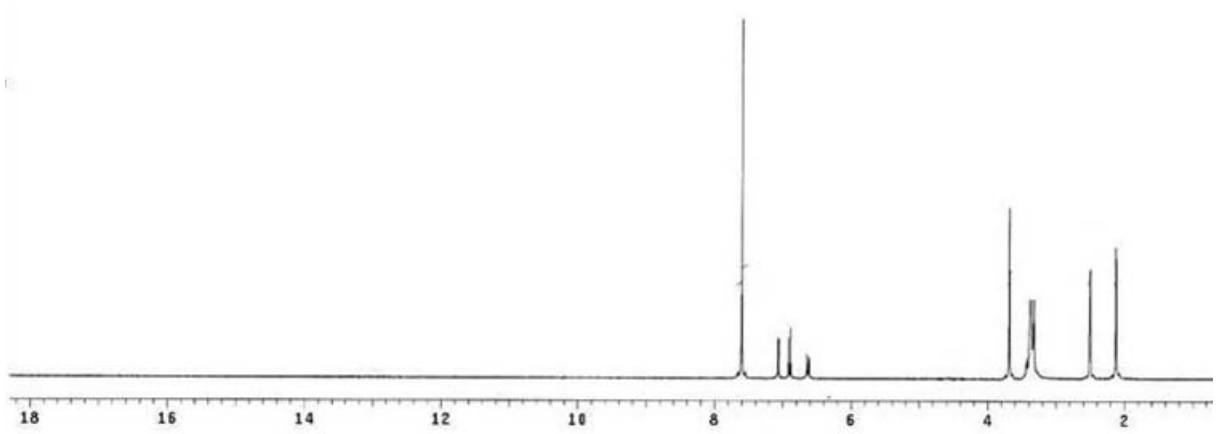

Fig. 3 – ^{1}H-NMR spectrum of Sr/*indo* complex.

Table 3

^{1}H-NMR spectral data of *indo* and its Sr(II) complex

Compound	δ ppm of hydrogen				
	2H; CH_2	3H; CH_3	3H; CH_3O	5H; ArH	H; COOH
indo-H	2.10	3.50	4.10	6.15-7.15	11.10
Sr(II)	2.12	3.43	3.68	6.61-7.60	--

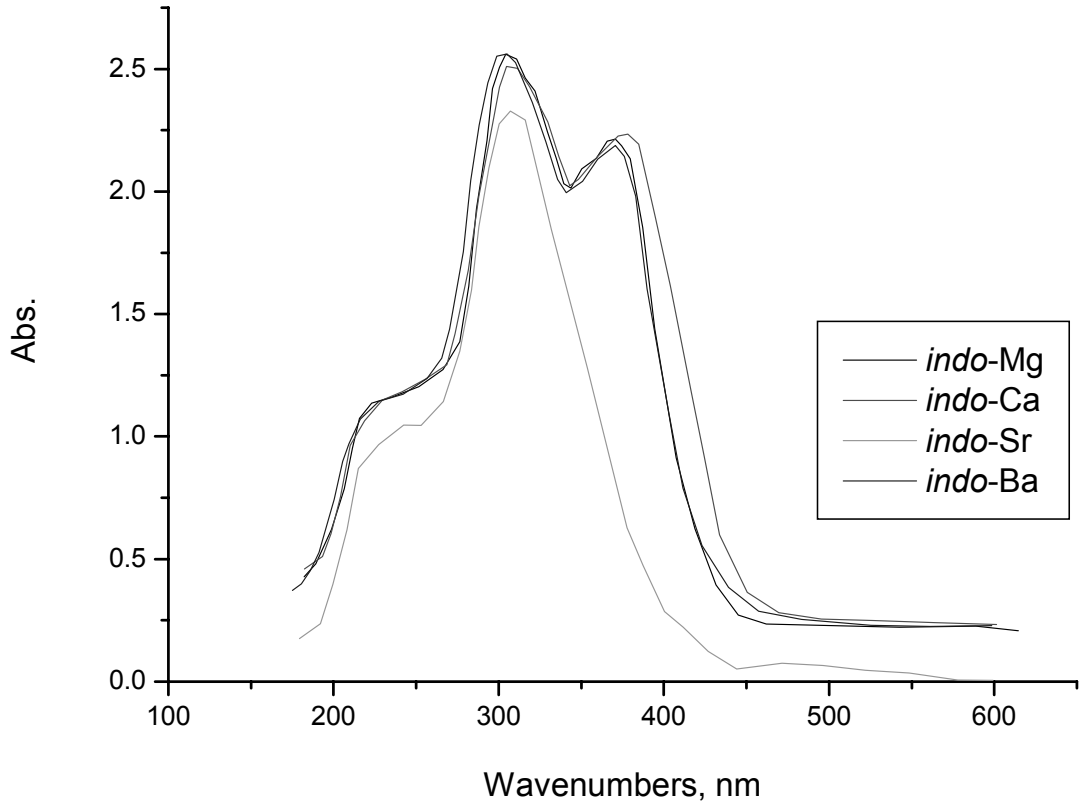

Fig. 4 – UV-vis spectra of *indo* complexes.

Optical absorption studies in the wavelength range of 200-600 nm at room temperature show that optical band gap E_g of *indo*-Mg, *indo*-Ca, *indo*-Sr and *indo*-Ba metal complex is 2.43, 2.53, 2.60, and 2.43 eV, respectively. The band gap energy can be calculated using Tauc model, in direct band transition case:[13]

$$(\alpha h\upsilon)^2 = A_o (h\upsilon - E_g)$$

where A_o is a constant, hυ is the photon energy and E_g is the optical band gap energy, α is optical absorption coefficient deduced from the absorption data. The optical energy band gap calculated from Tauc's plot (Fig. 5) varies from 2.43 eV to 2.60 eV, according to the metal type. The decrease in the band gap is attributed to the type of metal complexes. The results of optical study reported in this paper are in good agreement with the observations of other researchers.

In literature study[14] it is suggested that coordination leads to raised mobilization of the ligand electrons by accepting them in the shell of metal ions. It can be evaluated that after formation of the complex, the chemical structure of the ligands is changed, the width of the localized levels is expanded and, in turn, the band gap is smaller. This result is very significant in applications of electronic and optoelectronic devices, because of the lower optical band gap of the materials.[15] Small band gap facilitates electronic transitions between the HOMO-LUMO energy levels and makes the molecule more electro-conductive.[16] In essence, the obtained band gap values suggest that these complexes are semiconductors and lie in the same range of highly efficient photovoltaic materials. So, the present compounds could be considered potential materials for harvesting solar radiation in solar cell applications.[17] Perhaps, the little in the optical band gap Eg values between respected complexes is due to their same chemical structures.

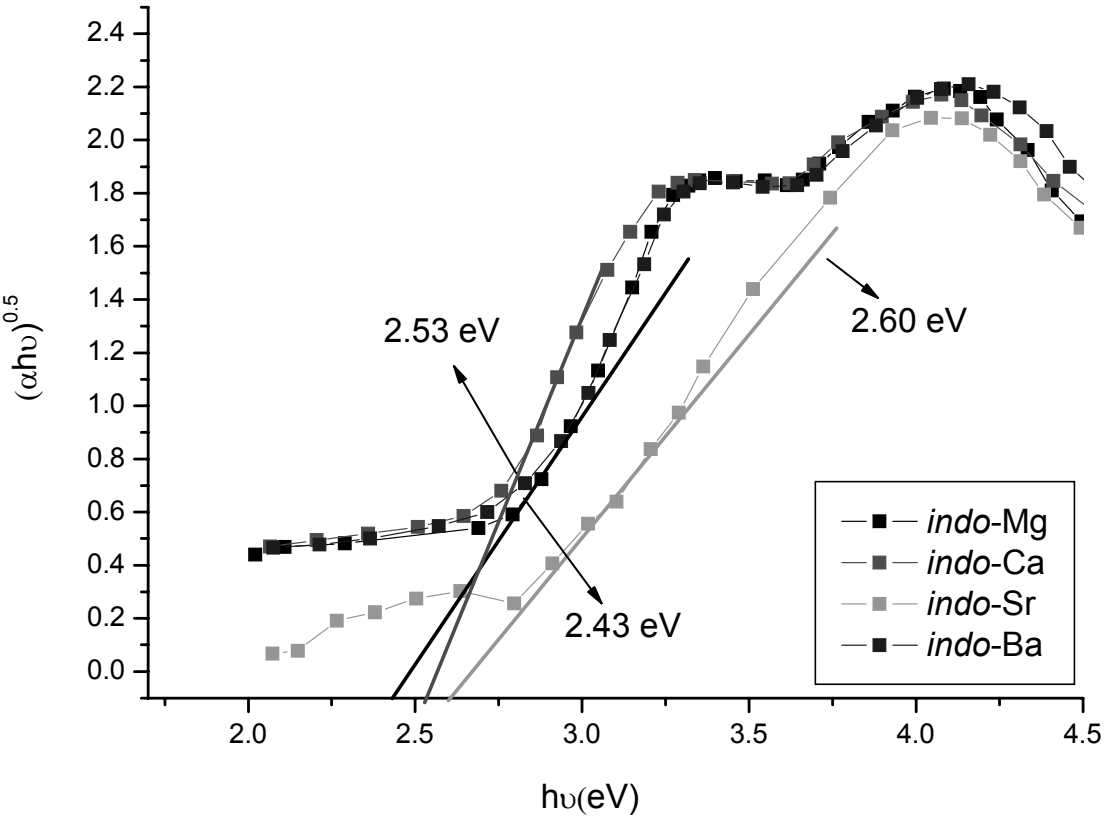

Fig. 5 – Optical absorbance spectra versus wavelength and plot of $(\alpha h\upsilon)^2$ *versus* $(h\upsilon)$ of *indo* complexes.

5. Thermogravimetric analyses

Thermal analysis curves (TG and DTG) of Mg(II), Ca(II), Sr(II) and Ba(II) *indo* complexes are shown in Fig. 6 and interpreted in Table 4.

The thermal decomposition of Sr(II)-*indo* complex occurs in three steps. The first degradation step takes place in the range of 80-300 ^{o}C and it corresponds to the eliminated of three coordinate H_2O molecules. The second step occurs in the range of 312-490 °C which is assigned to loss of $H_2O+C_8H_{15}O_2N_2Cl$. The third decomposition step within the temperature range (490-600 °C) assigned to loss of $C_{33}H_{15}O_5Cl$. The final product, formed at 700 °C, consists of (SrO with contaminated aromatic condensed phase).

The thermal decomposition of Ba(II)-*indo* complex proceeds with three degradation steps. The first decomposition stage occurs with maximum rate at temperature 291 °C. The mass loss at this step is associated with the loss of $4H_2O+C_8H_{20}$. The second decomposition stage occurs with maximum rate at temperature 444 °C, the observed mass loss of this step is associated with the loss of $C_8H_{10}O_4N_2Cl_2$. The third step of the degradation occurs at maximum temperature of 520 °C and is accompanied by loss of 3CO. The final product formed at 700 °C consists of BaO with contaminated aromatic condensed phase.

The thermal decomposition of Ca-*indo* complex has three decomposition steps. These steps located in the range between 80-200 °C, 200-500 °C and 500-650 °C and the mass loss for the first step is due to the loss of $4H_2O$. The second decomposition stage occurs with maximum rate at temperature 226 °C the mass loss at this step is associated with the loss of $C_{10}H_{30}O_3N$. The third step of the degradation occurs at maximum temperature of 598 °C and is accompanied by loss of $C_{25}O_4NCl_2$. The final product formed at 700 °C consists of (CaO with contaminated aromatic condensed phase).

The thermal decomposition of Mg(II)-*indo* complex occurs in four decomposition steps. The first degradation step takes place in range of 100-320 °C and it corresponds to the loss of $4H_2O+CH_4$. The second step occurs in the range of 320-400 °C which is assigned to loss of $C_6H_{12}O_4$. The third step occurs in the range of 400-490 °C which is assigned to loss of Cl_2. The fourth decomposition step occurs in the range of 490-600 °C which corresponds to the loss of $C_{19}H_{18}N_2O_3$. The final product formed at 700 °C consists of (MgO with contaminated aromatic condensed phase).

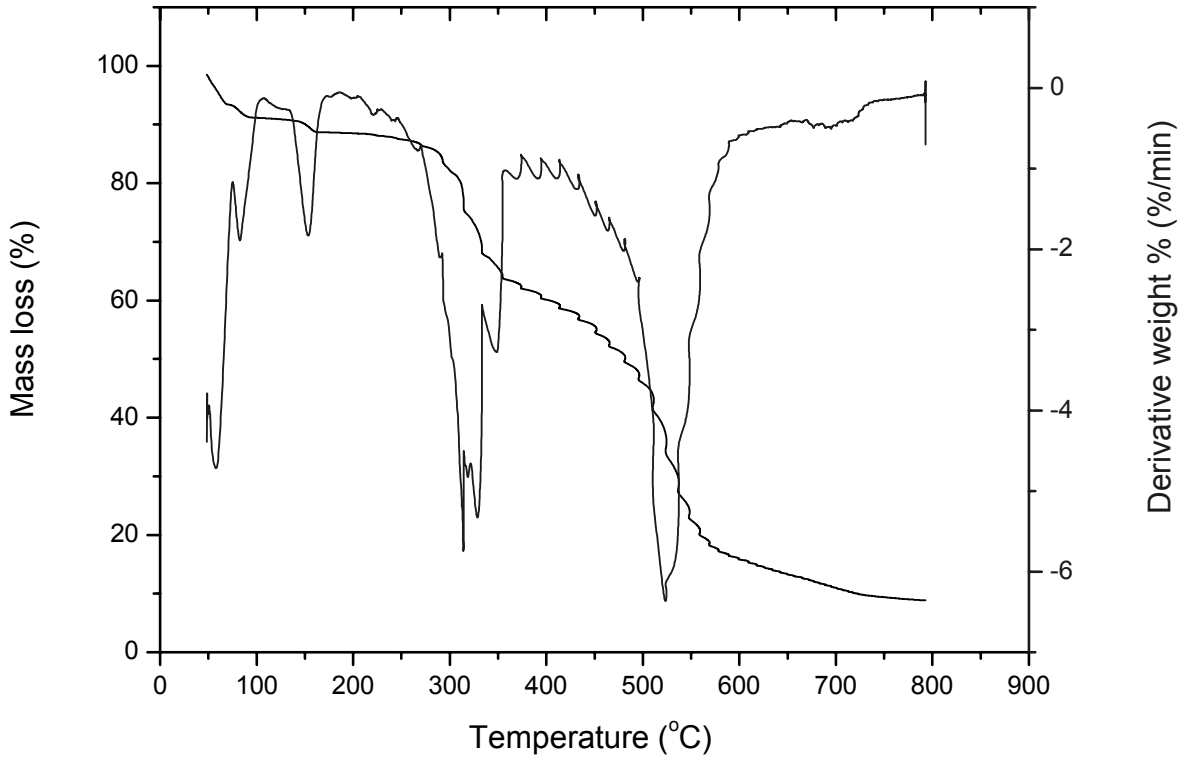

Fig. 6 – TG-DTG curve of *indo*-Ca(II) complex.

Table 4

Thermal analysis (TG) data summary for the synthesized *indo* complexes

Complexes	Steps	Temp range/(°C)	DTG peak /(°C)	TGA Mass loss %		Assignment
				Calcd.	Found	
1	1	80-312	206	6.10	5.80	$3H_2O$
	2	312-490	372	25.70	25.20	$H_2O+C_8H_{15}O_2N_2Cl$
	3	490-600	549	46.50	46.90	$C_{23}H_{15}O_5Cl$
						SrO+ aromatic condensed phase residual
2	1	100-375	291	20.40	20.50	$C_8H_20+4H_2O$
	2	375-477	444	29.10	28.90	$C_8H_{10}O_4N_2C_{l2}$
	3	477-650	520	9.10	9.10	3CO
						BaO+ aromatic condensed phase residual
3	1	80-200	128	8.70	9.40	$4H_2O$
	2	200-500	226	25.60	25.05	$C_{10}H_{30}O_3N$
	3	500-650	598	54.40	54.80	$C_{25}O_4NC_{l2}$
						CaO+ aromatic condensed phase residual
4	1	100-320	297	10.80	10.90	$4H_2O+CH_4$
	2	320-400	334	18.30	18.20	$C_6H_{12}O_4$
	3	400-490	443	8.70	8.60	Cl_2
	4	490-600	516	34.30	33.90	$C_{15}H_{18}N_2O_3$
						MgO+ aromatic condensed phase residual

6. Kinetic thermodynamic calculations

The kinetic and thermodynamic parameters have been evaluated using the Coats-Redfern and Horowitz-Metzger equations[18,19] (see Table 5).

The entropy of activation, ΔS^*, was calculated. The activation enthalpy, ΔH^*, and Gibbs free energy, ΔG^*, were calculated from $\Delta H^* = E^* - RT$ and $\Delta G^* = \Delta H^* - T\Delta S^*$, respectively[12,20]. The thermodynamic behavior of all the complexes of

indo with Mg(II), Ca(II), Sr(II) and Ba(II) metal ions is non-spontaneous (more ordered) reactions (ΔS is negative value), endothermic reactions (ΔH >0) and endergonic (ΔG >0) during the reactions. The thermodynamic data obtained with the two methods are in accordance with each other. The smaller size of the ions permits a closer approach of the ligand. Hence, the E value in the first stage for the Mg^{+2} complex is higher than that for the other Ba^{+2} complex. The correlation coefficients of the Arrhenius plots of the second step of the thermal decomposition were found to lie in the range 0.98 to 0.99, showing a good fit with linear function. It is clear that the thermal decomposition process of all *indo* complexes is non-spontaneous.[20]

7. Transmission electron microscopy

The surface morphological study and particle size of the *indo* complexes nanoparticles are carried out using TEM images. Figure 7 shows the TEM images of the prepared *indo*-Mg(II) complex in nanoparticles state within scale range 50-500 nm. It is evident that the *indo* complexes are formed from extremely semi-spherical particles which are loosely aggregated.

Table 5

Kinetic parameters based on Coats–Redfern (CR) and Horowitz–Metzger (HM) relationship for the *indo* complexes **1-4**

Complexes	Stage	Method	Parameter					r
			E (J mol^{-1})	A (s^{-1})	ΔS (J mol^{-1} K^{-1})	ΔH (J mol^{-1})	ΔG (J mol^{-1})	
1	2nd	CR	2.38×10^{5}	1.05×10^{17}	-9.21×10	2.30×10^{5}	1.74×10^{5}	0.9951
		HM	2.43×10^{5}	4.03×10^{17}	-1.00×10^{2}	2.32×10^{5}	1.72×10^{5}	0.9987
2	2nd	CR	9.31×10^{4}	6.41×10^{12}	-2.01×10	8.33×10^{4}	8.95×10^{4}	0.9923
		HM	9.22×10^{4}	5.90×10^{12}	-2.02×10	8.00×10^{4}	8.88×10^{4}	0.9932
3	2nd	CR	8.87×10^{4}	1.10×10^{7}	-1.10×10^{2}	8.43×10^{4}	1.40×10^{5}	0.9910
		HM	9.77×10^{4}	2.11×10^{7}	-9.21×10^{1}	9.64×10^{4}	1.44×10^{5}	0.9899
4	2nd	CR	6.09×10^{4}	4.71×10^{7}	-9.92×10^{1}	5.99×10^{4}	9.21×10^{4}	0.9954
		HM	6.01×10^{4}	3.62×10^{7}	-1.02×10^{2}	5.62×10^{4}	8.80×10^{4}	0.9963

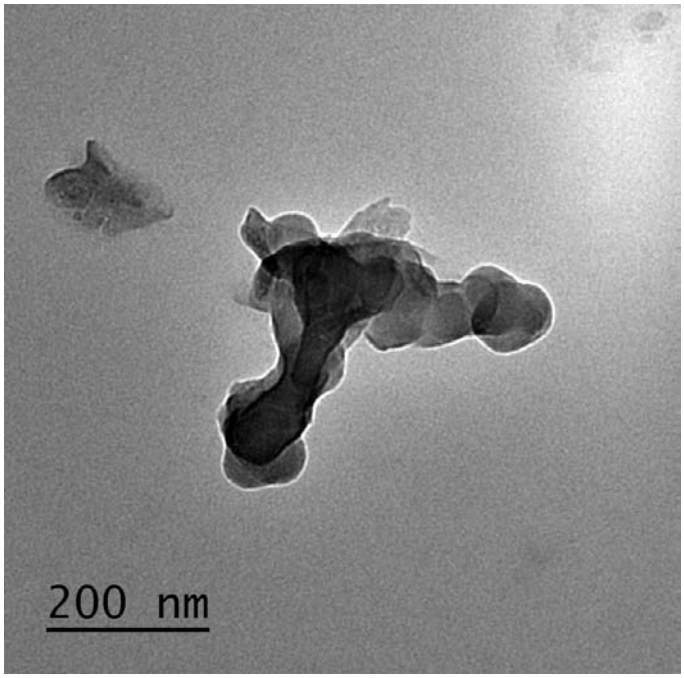

Fig. 7 – TEM image of *indo*-Mg(II) complex.

Table 6

Antimicrobial data of *indo* complexes

Samples	Diameter of inhibition zone (cm)			
	B. subtilis	*E. coli*	*Aspergillus niger*	*Aspergillus flavus*
Control	0	0	0	0
1	2.6	1.2	2	2.2
2	2.7	1.3	2.7	3.2
3	1.8	1.1	2.3	2.1
4	2.5	1.2	2.2	1.6

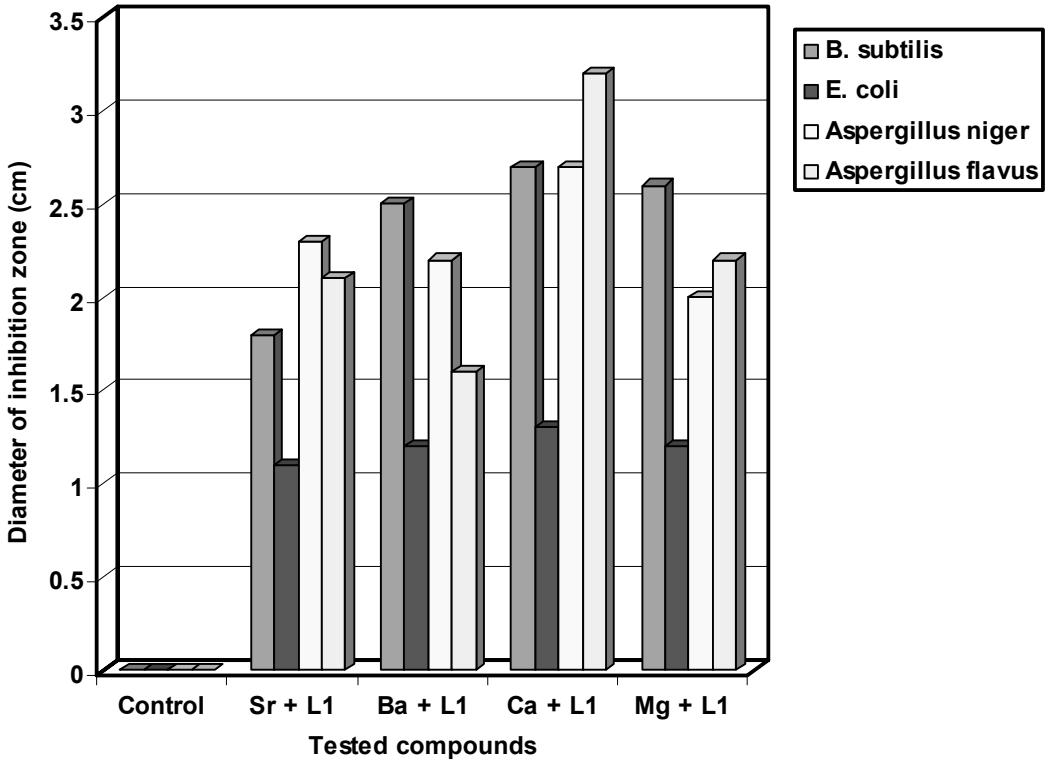

Fig. 8 – The diameter of inhibition zone (cm) for biological activity of *indo* (L1) complexes.

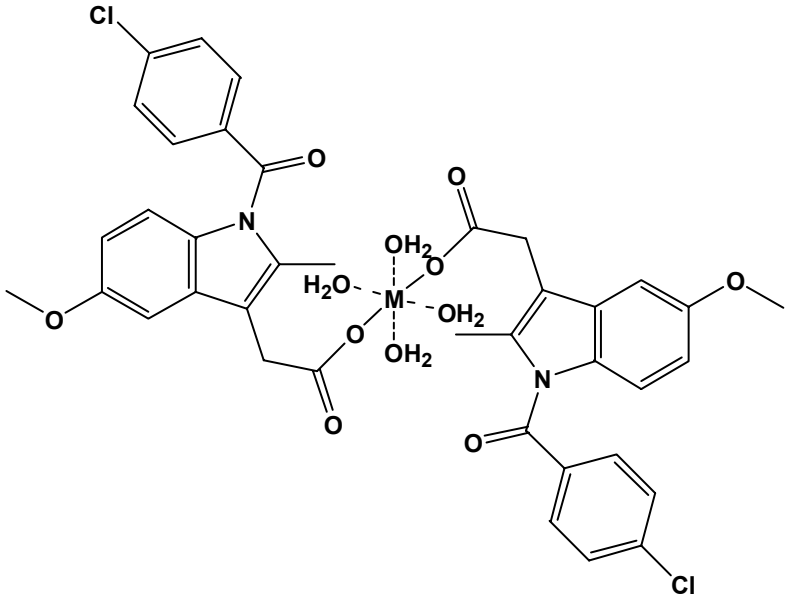

Fig. 9 – Suggested structure of indo complexes (M= Mg(II), Ca(II), Sr(II) and Ba(II)).

8. Antimicrobial activity

From Fig. 8 and Table 6, it can be seen that mean diameter of inhibition zone increased in the following order: Ca(II)-*indo* = Mg(II)/*indo* (1.3-2.7 cm) higher than Ba(II)-*indo* = Sr(II)/*indo* (1.2-2.5 cm) against four kinds of bacteria and fungi (*B. subtilis* (Gram, +ve), *Escherichia coli* (Gram, -ve) and fungal (*Aspergillus niger* and *Aspergillus flavus*) inhibitory zone. The high sensitivity of the *indo* complexes has been attributed to hyper conjugation of the coordinated aromatic Lewis bases, which increase the net electron density on the coordination metal(II) ion and consequently higher antimicrobial activity. The control sample (DMSO solvent) has not any influence on the inhibition zone of four kinds of bacteria and fungi as shown in Fig. 8.

9. Suggested structures of indo complexes

On the basis of the above interpretations, the following structures of Mg(II), Ca(II), Sr(II) and Ba(II) *indo* complexes may be suggested as referred in Fig. 9.

EXPERIMENTAL

1. Chemical and reagents

All chemicals were of reagent grade and were used without further purification. Indomethacin free drug was received from Aldrich Company and metal salts ($MgCl_2$, $SrCl_2$, $CaCl_2$ and $BaCl_2$) were purchased from Fluka.

2. Synthesis of Mg^{2+}, Sr^{2+}, Ca^{2+} and Ba^{2+} complexes

The *indo* complexes were synthesized by the reaction of divalent metal(II) chloride (1 mmol; 20 mL distilled water) to solution of *indo* (2 mmol; 20 mL 99% CH_3OH) with a stoichiometry of 1:2 (M:L). The pH was adjusted in between 7-8 using 5% NH_4OH in CH_3OH. The resulting solutions were stirred and refluxed on hot plate at 60 °C for 2 hrs. The resulted precipitates were filtered, washed several times with distilled H_2O to remove un-reacted ions from filtrate. The complexes resulted have low solubility in water and in common organic solvents and are well soluble in DMSO. The analytical data are in a good agreement with the proposed stoichiometry of the synthesized complexes.

3. Instruments

The elemental analyses of %C, %H and %N contents were performed by the microanalysis unit using a Perkin Elmer CHN 2400. The metal ions content has been determined using inductively coupled plasma mass spectrometry (ICP-MS). The molar conductivity of freshly prepared 10^{-3} mol/cm^3 dimethylsulfoxide (DMSO) solution was measured for the dissolved complexes using Jenway 4010 conductivity meter. The electronic spectra were measured on UV-3101 PC, Shimadzu, UV–Vis Spectrophotometer. The infrared spectra with KBr discs were recorded on a Bruker FT-IR Spectrophotometer (4000–400 cm^{-1}). ^{1}H-NMR spectra were scanned using a Varian Gemini 200 MHz Spectrometer. The solvent used was DMSO. The thermal study TG/DTG–50H was carried out on a Shimadzu thermogravimetric analyzer under nitrogen atmosphere till 800 °C. The transmission electron microscopy images were performed using JEOL 100s microscopy.

4. Antimicrobial effects

Antimicrobial activity of the tested samples was determined using a modified Kirby-Bauer disc diffusion method.[21] Briefly, 100 µL of the test bacteria/fungi were grown in 10 mL of fresh media until they reached a count of approximately 10^7 cells/ml for bacteria or 10^5 cells/ml for fungi.[22] 100 µL of microbial suspension was spread onto agar plates corresponding to the broth in which they were maintained. Isolated colonies of each organism that might be playing a pathogenic role should be selected from primary agar plates and tested for susceptibility by disc diffusion method.[23,24] Of the many media available, NCCLS recommends Mueller-Hinton agar due to: it results in good batch-to-batch reproducibility. Disc diffusion method for filamentous fungi tested by using approved standard method (M38-A) developed for evaluating the susceptibilities of filamentous fungi to antifungal agents.[25] Plates inoculated with filamentous fungi *as Aspergillus flavus* at 25°C for 48 hours; Gram (+) bacteria as *B. subtilis*; Gram (-) bacteria as *Escherichia coli* were incubated at 35-37°C for 24-48 hours, then the diameters of the inhibition zones were measured in millimeters.[21] The biological activity of Mg^{2+}, Sr^{2+}, Ca^{2+} and Ba^{2+} complexes of *indo* drugs were tested against bacteria and fungi. In testing the antibacterial activity of these complexes, we used more than one test organism. The organisms used in the present investigation included two bacteria *B. subtilis* (Gram +ve), *E. coli* (Gram –ve) and two fungi *Aspergillus niger* and *Aspergillus flavus*. The results of the bactericidal screening and fungicidal of the synthesized complexes were collected.

CONCLUSION

In summary, four mononuclear M(II) complexes, $[M(L)_2(H_2O)_4]$ (M= Mg(II), Ca(II), Sr(II) and Ca(II)) were synthesized and characterized by elemental analysis, FTIR, ^{1}HNMR and electronic spectra, TG/DTG, molar conductivity and elemental measurements. The Indo drug acts to M(II) as monodentate donor. The thermal stability of synthesized complexes was investigated based on the TG/DTG and calculated thermodynamic parameters. Morphological surfaces of *Indo* complexes located within the nanoscale range. The results of the biological evaluation revealed the antimicrobial efficiency against G(+) and G(-) bacteria as well as two fungal species (*Aspergillus niger* and *Aspergillus flavus*).

REFERENCES

1. G. Augeliki, K.D. Dimitra and K. Nikotaos, *Polyhedron*, **2004,** *23*, 2012.
2. S. Auilk and Hardeepwadhwa, *Int. J. Pharm*., **1995**, *120*, 145.
3. M. Kirkova, T. Kassabova and E. Ruissaua, *J. Pharm*., **1992**, *23*, 811.

4. J.R. Vane, R.M. Botting and Semin, *Arthritis Rheum*., **1997**, *26*, 2.
5. J.E. Weder, T.W. Hambley, B.J. Kennedy and P.A. Lay, *Inorg. Chem*., **1999**, *38*, 1736.
6. J.E. Weder, C.T. Dillon, T.W. Hambley, B.J. Kennedy, P.A., Lay, J.R. Biffin, H.L. Regtop and N.M. Davis, *Coord. Chem. Rev*., **2002**, *232*, 95.
7. K.R. Jisha, S. Suma and M.P. Sudarsankumar, *Polyhedron*, **2010**, *2*, 3104.
8. K. Burger, "Coordination Chemistry: Experimental Method", Butterworth group, Britain, 1973.
9. R.M. Ying, T. Peter, H.K. Brendan and H. Trevorw, *Inorg. Chim. Acta*, **2001**, *324*, 150.
10. S. Jombhekar, R. Casella and T. Moher, Int. J. Pharm., **2004**, *270*, 149.
11. K. Nakamato, "Infrared and Raman Spectra of Inorganic and Coordination Compound", 3rd edition, John Wiley & Sons, Inc., New York, 1978.
12. M.S. Refat, H.M.A. Killa, A.F. Mansour, M.Y. Ibrahim and H. Fetooh, *J. Chem. Eng. Data*, **2011**, *56*, 3493.
13. J. Tauc, *Mater. Res. Bull*. **1968**, *3*, 37.
14. F Karipcin, B Dede, Y Caglar, D Hur, S Ilican, M Caglar and Y Sahin, *Opt. Commun*., **2007**, *272*, 131.
15. N. Turan, B. Gündüz, H. Körkoca, R. Adigüzel, N. Çolak and K. Buldurun, *J. Mex. Chem. Soc*., **2014**, *58*, 65.
16. S.K. Sengupta, O.P. Pandey, B.K. Srivastava and V. Sharma, *Trans. Met. Chem*., **1998**, *23*, 349.
17. M.L. Fu, G.C. Guo, X. Liu, L.Z. Cai and J.S. Huang, Inorg. *Chem. Commun*., **2005**, *8*, 18.
18. A.W. Coats and J.P. Redfern, Nature, **1964**, *201*, 68.
19. H.W. Horowitz and G. Metzger, *Anal. Chem*., **1963**, 35, 1464.
20. P.B. Maravalli and T.R. Goudar, Thermochim. Acta, **1999**, *325*, 35.
21. A.W. Bauer, W.M. Kirby, C. Sherris and M. Turck, *Am. J. Clin. Path*., **1966**, *45*, 493.
22. M.A. Pfaller, L. Burmeister, M.A. Bartlett and M.G. Rinaldi, *J. Clin. Microbiol*. **1988**, *26*, 1437.
23. National Committee for Clinical Laboratory Standards. 1993. Methods for dilution antimicrobial susceptibility tests for bacteria that grow aerobically. Approved standard M7-A3. National Committee for Clinical Laboratory Standards, Villanova, Pa.
24. National Committee for Clinical Laboratory Standards. 1997. Performance VOL. 41, antimicrobial susceptibility of Flavobacteria.
25. National Committee for Clinical Laboratory Standards. (2002). Reference Method for Broth Dilution Antifungal Susceptibility Testing of Conidium-Forming Filamentous Fungi: Proposed Standard M38-A. NCCLS, Wayne, PA, USA.